Vol 455|9 October 2008|doi:10.1038/nature07293

LETTERS

High-temperature interface superconductivity between metallic and insulating copper oxides

A. Gozar[1], G. Logvenov[1], L. Fitting Kourkoutis[2], A. T. Bollinger[1], L. A. Giannuzzi[3], D. A. Muller[2] & I. Bozovic[1]

The realization of high-transition-temperature (high-T_c) superconductivity confined to nanometre-sized interfaces has been a long-standing goal because of potential applications[1,2] and the opportunity to study quantum phenomena in reduced dimensions[3,4]. This has been, however, a challenging target: in conventional metals, the high electron density restricts interface effects (such as carrier depletion or accumulation) to a region much narrower than the coherence length, which is the scale necessary for superconductivity to occur. By contrast, in copper oxides the carrier density is low whereas T_c is high and the coherence length very short, which provides an opportunity—but at a price: the interface must be atomically perfect. Here we report superconductivity in bilayers consisting of an insulator (La_2CuO_4) and a metal ($La_{1.55}Sr_{0.45}CuO_4$), neither of which is superconducting in isolation. In these bilayers, T_c is either ~15 K or ~30 K, depending on the layering sequence. This highly robust phenomenon is confined within 2–3 nm of the interface. If such a bilayer is exposed to ozone, T_c exceeds 50 K, and this enhanced superconductivity is also shown to originate from an interface layer about 1–2 unit cells thick. Enhancement of T_c in bilayer systems was observed previously[5] but the essential role of the interface was not recognized at the time.

Typical approaches to the realization of quasi-two-dimensional superconducting sheets rely on fabrication of an 'ultrathin' layer of a known superconductor[1,2]. Another route is to use hetero-interfaces. Superconductivity in the 0.2–6 K range was reported at the interface between two oxide insulators[6] and in superlattices where one[7] or both[8] components are semiconductors. The $La_{2-x}Sr_xCuO_4$ (LSCO) family is particularly attractive because these materials are solid solutions that can be doped over a broad range[9].

In our experiment, we have synthesized a large number (over 200) of single-phase, bilayer and trilayer films with insulating (I), metallic (M) and superconducting (S) blocks in all combinations and of varying layer thickness (for notation, see Fig. 1 legend). The films were grown in a unique atomic-layer-by-layer molecular beam epitaxy system[10] that incorporates *in situ* state-of-the-art surface science tools, such as time-of-flight ion scattering and recoil spectroscopy, and reflection high-energy electron diffraction. It enables synthesis of atomically smooth films as well as multilayers with perfect interfaces[5,11–13]. Typical surface roughnesses determined from atomic force microscopy data are 0.2–0.5 nm, less than one unit cell, which in LSCO is 1.3 nm. Atomic-layer-by-layer molecular beam epitaxy provides for digital control of layer thickness, which we measure by counting the number of unit cells. Maintaining atomic-scale smoothness and digital layer-by-layer growth are both crucial for the results we discuss in the following.

The interface between the metallic and insulating materials is superconducting with high T_c (Fig. 1), and the deposition sequence matters. M–S bilayers show the highest T_c, ~50 K. In contrast, in single-phase LSCO films that we have grown under the same conditions, the highest T_c is about 40 K, similar to what is seen in bulk single crystals (ref. 9 and Supplementary Fig. 1). Hence, in M–S bilayers we see a large (up to 25%) relative T_c enhancement. T_c values around 50 K were observed previously in some LSCO films[14,15] and

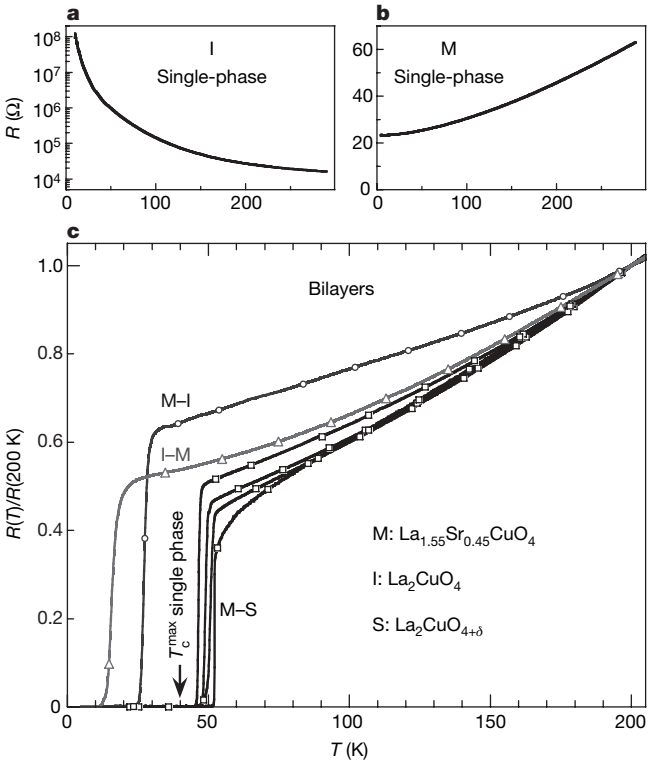

Figure 1 | The dependence of resistance on temperature for single-phase and bilayer films. Notation used in text and figures is as follows: I is La_2CuO_4, vacuum-annealed and insulating; S is $La_2CuO_{4+\delta}$, oxygen-doped by annealing in ozone and superconducting; M is $La_{1.55}Sr_{0.45}CuO_4$, overdoped and metallic but not superconducting; *R*, resistance; *T*, temperature. For bilayers, the first letter always denotes the layer next to the $LaSrAlO_4$ substrate. **a**, **b**, $R(T)$ for single-phase layers of I (**a**; note the log scale) and M (**b**). **c**, $R(T)$ normalized to $T = 200$ K for various bilayers. Typical values for T_c at the mid-point of the resistive transitions are $T_c \approx 15$ K in I–M and $T_c \approx 30$ K in M–I structures. In M–S bilayers (four samples shown), $T_c \approx 50$ K. In a few hundred single-phase films (doped by either oxygen or Sr) grown under the same conditions, T_c never exceeded 40 K, the value marked by the arrow (Supplementary Fig. 1). The interface superconductivity is reproducible and stable in air on the scale of months in contrast to single-phase S films.

[1]Brookhaven National Laboratory, Upton, New York 11973-5000, USA. [2]School of Applied and Engineering Physics, Cornell University, Ithaca, New York 14853, USA. [3]FEI Company, Hillsboro, Oregon 97124, USA.

LSCO–LCO bilayers[5], but the locus of the highest T_c has not been investigated. We show below that in our M–I films, enhanced superconductivity originates from and is restricted to an interfacial layer 1–2 unit cells thick. In retrospect, one would suppose that at least the bilayer result[5] was also an interface effect, a proposition that we confirmed, as discussed below.

To directly determine the length scale associated with interface superconductivity, we synthesized a series of M–I and I–M structures with thick bottom layers (≥30 unit cells) while the thickness of the top layer was increased digitally, one-half a unit cell at a time (Fig. 2). The transport data show that the plateau values for superconductivity are reached after the thickness of the top layer is ≥2 unit cells, a value that sets the length scale for this interface phenomenon.

The T_c enhancement in M–S bilayers triggers the intriguing question as to whether this enhancement is an interface phenomenon, as suggested by several preliminary observations (Supplementary Information). That this is the case is confirmed by the data on critical current density (j_c) determined from two-coil mutual inductance measurements[16–18] (Fig. 3). The results indicate that the $T_c \approx 50$ K in M–S structures is in fact confined to a very thin (1–2 unit cells thick) layer near the interface. The observed linear temperature dependence of j_c in S films is expected theoretically in copper oxides for the intrinsic critical current due to vortex–antivortex pair breaking or depinning in homogeneous samples[19], and it is observed experimentally in high-quality films and bulk single crystals of high-temperature superconductors[20]. In contrast, in M–S samples, one can see a clear break near 40 K that separates two approximately linear regions with very different slopes.

This is what one expects from two superconducting sheets with different thicknesses and transition temperatures, say d_1, T_{c1} and d_2, T_{c2}, respectively. The breakdown into two such components (the dashed lines in Fig. 3) provides $T_{c1} \approx 40$ K and $T_{c2} \approx 50$ K. The

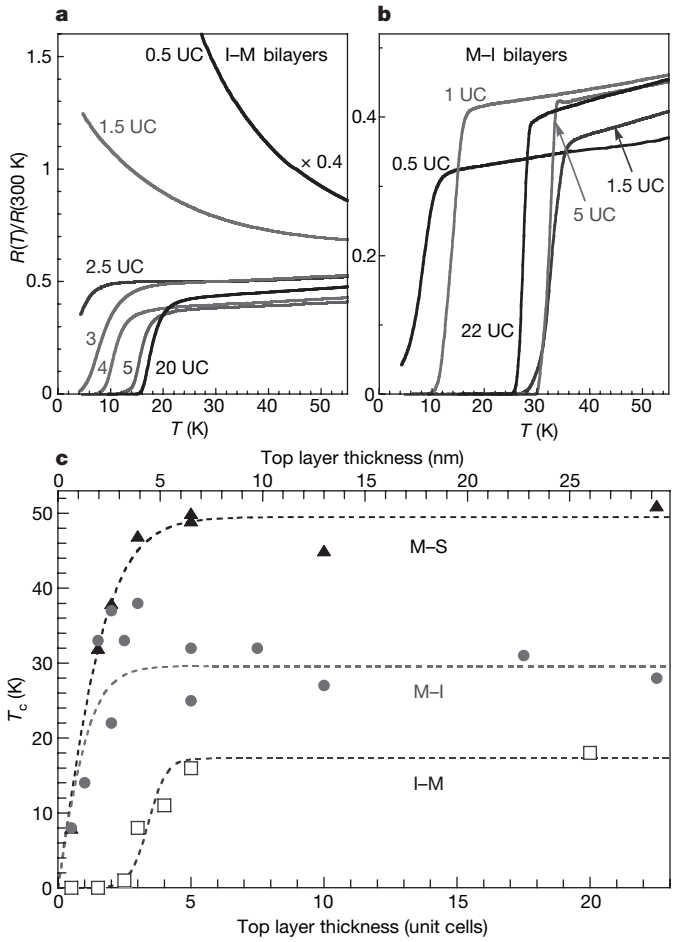

Figure 2 | The dependence on the layer thickness. a, Normalized resistance for several I–M bilayers where the thickness of the bottom I layer is fixed at 40 unit cells, that is, 52 nm, and the thickness of the M layer is varied as indicated (UC, unit cell). For an M layer 0.5 unit cells thick the sample is insulating, whereas the 1.5 unit cell structure shows a metallic-to-insulating crossover near $T = 75$ K. Further increase of the thickness raises T_c to a plateau of 15 K. **b**, The same for M–I bilayers with a 40-unit-cell-thick bottom M layer. Traces of superconductivity can be observed even when the bottom M layer is covered by an I layer only 0.5 unit cell thick (0.66 nm). When one unit cell of I covers the surface, the resistive transition is complete and $T_c > 10$ K. On its own, this is a signature of virtually atomically perfect surfaces, given that the resistance measurements were taken with the voltage probes 3 mm apart. **c**, T_c (defined as the midpoint of the resistive transition) as a function of the top layer thickness in M–I, I–M and M–S bilayers. The last are structures obtained by annealing M–I bilayers in an ozone atmosphere, the procedure that turns I films into S but has essentially no effect on M. Dashed lines are guides for the eye.

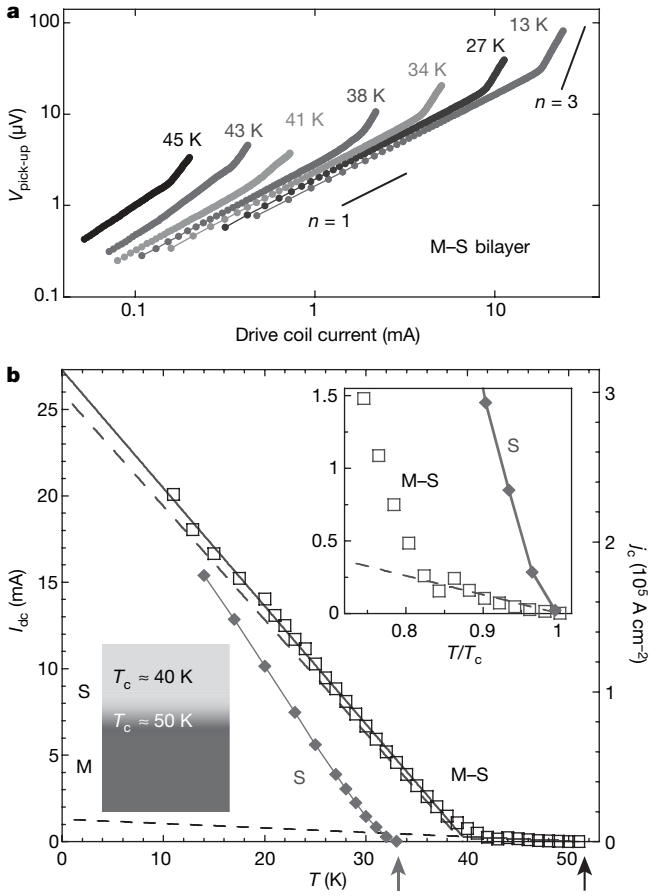

Figure 3 | Nonlinear screening effects in a single-phase S film and an M–S bilayer. a, The dependence of the pick-up voltage on the current in the drive coil at several temperatures. At each temperature, a 'critical' value of the current in the drive coil, I_{dc}, corresponds to the onset of dissipation in the film, and can be defined as the crossover point between a linear ($n = 1$) and a higher-power law ($n \approx 3$ at temperatures below 40 K) behaviour. In both samples, the S layer is 20 unit cells thick. **b**, The temperature dependence of I_{dc} for an S film (filled diamonds) and an M–S bilayer (open squares). The right scale shows the calculated peak value of the induced screening current density in superconducting films (see also Supplementary Fig. 5). Arrows denote values of T_c: 33.2 K and 51.6 K for the S and M–S samples, respectively. The bilayer data can be well decomposed into two approximately linear contributions (dashed lines), corresponding to bulk and interface parts with $T_c \approx 40$ K and $T_c \approx 50$ K (lower left inset). Top right inset shows the same data in reduced temperature units, T/T_c. The magnitude of the estimated low-temperature critical current of the thin layer is in agreement with the value estimated from mutual inductance and transport measurements in M–I bilayers in which the high-temperature superconductor ($T_c = 30$ K) sheet has a similar thickness.

low-temperature extrapolation of the critical current gives $d_1/d_2 \approx 20$. As the total number of layers deposited was $d_1 + d_2 = 20$ unit cells, one obtains $d_2 \approx 1$ unit cell. This length scale is quantitatively consistent with the independent measurements of resistivity in M–S bilayers as a function of top layer thicknesses (Fig. 2c). We performed similar mutual inductance measurements on the same bilayer sample (which had not deteriorated after seven years) that was studied in ref. 5, in which the bottom layer was optimally doped LSCO, and the results were quite similar to the M–S case; this demonstrates that the previously reported T_c enhancement was also an interface effect.

We now consider the issue of interface structure and the possible impact of cation interdiffusion (Fig. 4). The microstructure of an M–I bilayer and its interfaces was analysed using electron energy-loss spectroscopy in a scanning transmission electron microscope. An upper limit on the amount of chemical interdiffusion at the interfaces is obtained by recording the lanthanum-$M_{4,5}$ edges in the spectra. The root-mean-square interface roughness, as determined by fitting error functions to the La profile, is $\sigma = 0.8 \pm 0.4$ nm at the substrate–M interface and $\sigma = 1.2 \pm 0.4$ nm ($\sim$1 unit cell) at the M–I interface, which sets an upper limit to any cation intermixing (see also Supplementary Fig. 8).

As an independent test of chemical variations across the interfaces, the changes in the oxygen-K fine structure were analysed using a principal-components analysis. The fraction of the component corresponding to the M layer is shown in Fig. 4d, which again indicates an interface roughness of less than one unit cell. Either interface was fully described by two components, leaving no significant residual after the fit, suggesting that there is no substantial third, interfacial layer, at least on the scale of the interface roughness. Results obtained by several other surface-sensitive probes, such as reflection high-energy electron diffraction, and time-of-flight ion scattering and recoil spectroscopy, as well as transport on I–M–I heterostructures (Supplementary Figs 2, 3 and 4), support and are consistent with the chemically abrupt interfaces inferred from the scanning transmission electron microscope data. The experiments set an upper limit on possible cation interdiffusion of less than 1 unit cell depth, and make the cation mixing scenario hard to reconcile quantitatively and qualitatively with our observations.

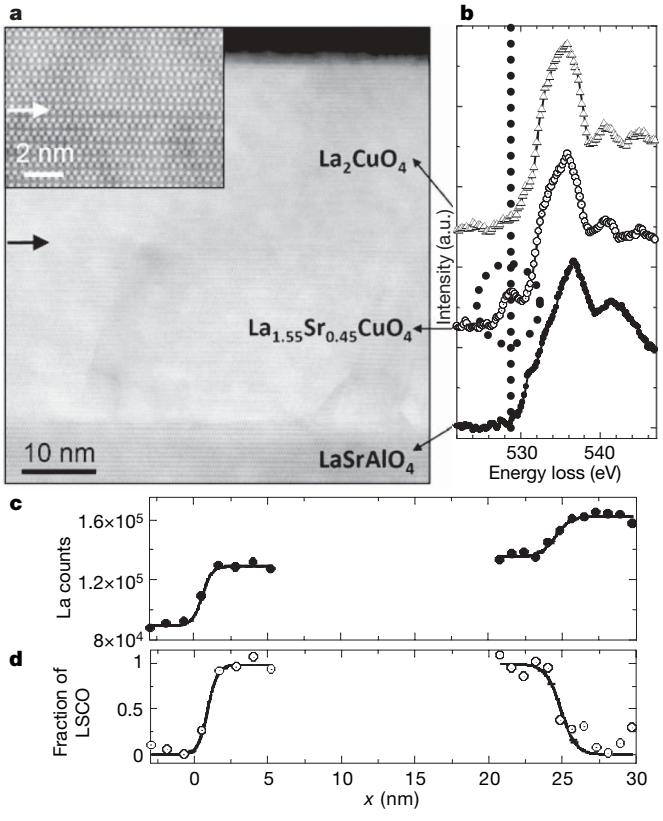

Figure 4 | Analysis of an M–I bilayer by scanning transmission electron microscopy and electron energy-loss spectroscopy. a, Annular dark field image of the structure (main panel). Inset, a magnified image of the M–I interface (arrowed). **b**, Oxygen-K (O-K) electron energy-loss spectra of the three oxides in the structure, showing clear changes in the fine structure of the O-K edge. For LSCO, an O-K edge pre-peak (circled) evolves for $x > 0$ and scales with the doping level[26,27]. a.u., arbitrary units. **c**, The integrated La intensity across the bilayer. As expected, the La profile shows an increase in the La concentration from the substrate to the M layer, and again from the M to the I layer. **d**, Results of a principal-components analysis of the two interfaces. The fraction of one of two components, corresponding to the O-K edge in $La_{1.55}Sr_{0.45}CuO_4$, is shown.

Other possible causes for the high-temperature superconductivity at the interface are electronic reconstruction or oxygen non-stoichiometry. Experimental data show that charge depletion or accumulation is substantial across M–I and I–M interfaces[21], whereas such charge transfer is negligible when M is replaced by optimally doped LSCO (ref. 15). These findings are consistent with the doping dependence of the chemical potential in LSCO inferred from X-ray photoemission data[22]. Oxygen vacancies and interstitials are nevertheless additional factors that should be considered: they may account for the asymmetry between M–I and I–M structures, and are essential for the increased T_c and stability of superconductivity in M–S bilayers (Supplementary Information, section E).

A remaining puzzle is the mechanism of relative T_c enhancement in M–S bilayers. It is conceivable that structural aspects, such as disorder, play a crucial role. We may have realized the doping without disorder scenario[23] by introducing carriers via charge transfer and by (ordered) interstitial oxygen pinned near the interface. Another possibility is that the 'intrinsic' T_c in LSCO would be even higher were it not for some competing instability, and that this other order parameter is suppressed in bilayers via the long-range strain or electrostatic effects (or both). Finally, an interesting possibility is that pairing and/or coherence of electrons in one layer is enabled or enhanced by interactions originating in the neighbouring layer[24,25]. Deciphering this problem may open the path to even larger T_c enhancement.

Received 15 June 2007; accepted 25 July 2008.

1. Ahn, C. H., Triscone, J.-M. & Mannhart, J. Electric field effect in correlated oxide systems. *Nature* **424,** 1015–1018 (2003).
2. Ahn, C. H. *et al.* Electrostatic modulation of superconductivity in ultrathin $GdBa_2Cu_3O_{7-\delta}$. *Science* **284,** 1152–1155 (1999).
3. Berezinskii, V. L. Destruction of long-range order in one-dimensional and 2-dimensional systems having a continuous symmetry group 2. Quantum systems. *Sov. Phys. JETP* **34,** 610–616 (1972).
4. Kosterlitz, J. M. & Thouless, D. J. Ordering, metastability and phase transitions in two-dimensional systems. *J. Phys. C* **6,** 1181–1203 (1973).
5. Bozovic, I., Logvenov, G., Belca, I., Narimbetov, B. & Sveklo, I. Epitaxial strain and superconductivity in $La_{2-x}Sr_xCuO_4$ thin films. *Phys. Rev. Lett.* **89,** 107001 (2002).
6. Reyren, N. *et al.* Superconducting interfaces between insulating oxides. *Science* **317,** 1196–1199 (2007).
7. Seguchi, Y., Tsuboi, T. & Suzuki, T. Magnetic-field-enhanced superconductivity in Au/Ge layered films. *J. Phys. Soc. Jpn* **61,** 1875–1878 (1992).
8. Fogel, N. Ya. *et al.* Interfacial superconductivity in semiconducting monochalcogenide superlattices. *Phys. Rev. B* **73,** R161306 (2006).
9. Kastner, M. A. & Birgeneau, R. J. Magnetic, transport and optical properties of monolayer copper oxides. *Rev. Mod. Phys.* **70,** 897–928 (1998).
10. Bozovic, I. Atomic layer engineering of superconducting oxides: Yesterday, today, tomorrow. *IEEE Trans. Appl. Supercond.* **11,** 2686–2695 (2001).
11. Bozovic, I., Eckstein, J. N. & Virshup, G. F. Superconducting oxide multilayers and superlattices: Physics, chemistry and nanoengineering. *Physica C* **235–240,** 178–181 (1994).
12. Bozovic, I. *et al.* No mixing of superconductivity and antiferromagnetism in a high temperature superconductor. *Nature* **422,** 873–875 (2003).
13. Gozar, A., Logvenov, G., Butko, V. B. & Bozovic, I. Surface structure analysis of atomically smooth $BaBiO_3$ films. *Phys. Rev. B* **75,** R201402 (2007).
14. Sato, H., Tsukada, A., Naito, M. & Matsuda, A. $La_{2-x}Sr_xCuO_y$ epitaxial films ($x = 0$ to 2): Structure, strain, and superconductivity. *Phys. Rev. B* **61,** 12447–12456 (2000).
15. Locquet, J.-P. *et al.* Doubling the critical temperature of $La_{1.9}Sr_{0.1}CuO_4$ using epitaxial strain. *Nature* **394,** 453–456 (1998).

16. Hebard, A. F. & Fiory, A. T. Evidence for the Kosterlitz-Thouless transition in thin superconducting aluminum films. *Phys. Rev. Lett.* **44,** 291–294 (1980).
17. Claassen, J. H., Reeves, M. E. & Soulen, R. J. Jr. A contactless method for measurement of the critical current density and critical temperature of superconducting rings. *Rev. Sci. Instrum.* **62,** 996–1004 (1991).
18. Clem, J. R. & Coffey, M. W. Vortex dynamics in a type-II superconducting film and complex linear-response functions. *Phys. Rev. B* **46,** 14662–14674 (1992).
19. Jensen, H. J. & Minnhagen, P. Two-dimensional vortex fluctuations in the nonlinear current-voltage characteristics for high-temperature superconductors. *Phys. Rev. Lett.* **66,** 1630–1633 (1991).
20. de Vries, J. W. C., Stollman, G. M. & Gijs, M. A. M. Analysis of the critical current density in high-T_c superconducting films. *Physica C* **157,** 406–414 (1989).
21. Smadici, S. *et al.* Hole delocalization in superconducting La_2CuO_4-$La_{1.64}Sr_{0.36}CuO_4$ superlattices. Preprint at ⟨http://xxx.lanl.gov/abs/0805.3189⟩ (2008).
22. Ino, A. *et al.* Chemical potential shift in overdoped and underdoped $La_{2-x}Sr_xCuO_4$. *Phys. Rev. Lett.* **79,** 2101–2104 (1997).
23. Fujita, K., Noda, T., Kojima, K. M., Eisaki, H. & Uchida, S. Effect of disorder outside the CuO_2 planes on T_c of copper oxide superconductors. *Phys. Rev. Lett.* **95,** 097006 (2005).
24. Ginzburg, V. L. On interface superconductivity. *Phys. Lett.* **13,** 101–102 (1964).
25. Kivelson, S. A. Making high T_c higher: A theoretical proposal. *Physica B* **318,** 61–67 (2002).
26. Romberg, H., Alexander, M., Nücker, N., Adelmann, P. & Fink, J. Electronic structure of the system $La_{2-x}Sr_xCuO_{4+\delta}$. *Phys. Rev. B* **42,** R8768–R8771 (1990).
27. Chen, C. T. *et al.* Electronic states in $La_{2-x}Sr_xCuO_{4+\delta}$ probed by soft-x-ray absorption. *Phys. Rev. Lett.* **66,** 104–107 (1991).

Supplementary Information is linked to the online version of the paper at www.nature.com/nature.

Acknowledgements The work at BNL was supported by US DOE. L.F.K. and D.A.M. acknowledge support under the ONR EMMA MURI and by the Cornell Center for Materials Research. L.F.K. acknowledges financial support by Applied Materials.

Author Contributions A.G. and G.L. contributed equally to this work. Film synthesis and characterization was by G.L and I.B.; transport and time-of-flight ion scattering and recoil spectroscopy was by A.G.; lithography was by A.T.B.; electron microscopy was by L.F.K. and supervised by D.A.M.; and TEM sample preparation was by L.A.G. and L.F.K.

Author Information Reprints and permissions information is available at www.nature.com/reprints. Correspondence and requests for materials should be addressed to I.B. (bozovic@bnl.gov).